Mechanism of Formation of a Productive Molten Globule Form of Barstar †

ARTICLE *in* BIOCHEMISTRY · MARCH 2002

Impact Factor: 3.02 · DOI: 10.1021/bi0120300 · Source: PubMed

2 AUTHORS, INCLUDING:

Jayant B Udgaonkar
Tata Institute of Fundamental Research
147 PUBLICATIONS **4,298** CITATIONS

SEE PROFILE

Mechanism of Formation of a Productive Molten Globule Form of Barstar[†]

Bhadresh R. Rami and Jayant B. Udgaonkar*

National Centre for Biological Sciences, Tata Institute of Fundamental Research, GKVK Campus, Bangalore 560065, India

Received November 6, 2001; Revised Manuscript Received December 13, 2001

ABSTRACT: Structural analysis of the initial steps in protein folding is difficult because of the swiftness with which these steps occur. Hence, the link between initial polypeptide chain collapse and formation of secondary and other specific structures remains poorly understood. Here, an equilibrium model has been developed for characterizing the initial steps of folding of the small protein barstar, which lead to the formation of a productive molten globule in the folding pathway. In this model, the high-pH-unfolded form (D form) of barstar, which is shown to be as unstructured as the urea-denatured form, is transformed progressively into a molten globule B form by incremental addition of the salt Na_2SO_4 at pH 12 . At very low concentrations of Na_2SO_4, the D form collapses into a pre-molten globule (P) form, whose volume exceeds that of the native (N) state by only 20%, and which lacks any specific structure as determined by far- and near-UV circular dichroism. At higher concentrations of Na_2SO_4, the P form transforms into the molten globule (B) form in a highly noncooperative transition populated by an ensemble of at least two intermediates. The B form is a dry molten globule in which water is excluded from the core, and in which secondary structure develops to 65% and tertiary contacts develop to 40%, relative to that of the native protein. Kinetic refolding experiments carried out at pH 7 and at high Na_2SO_4 concentrations, in which the rate of folding of the D form to the N state is compared to that of the B form to the N state, indicate conclusively that the B form is a productive intermediate that forms on the direct pathway of folding from the D form to the N state.

Molten globule-like folding intermediates, whether kinetic (*1*−*6*) or equilibrium (*7*−*11*), have been implicated as productive intermediates in the folding of many proteins, and their importance has been validated by many theoretical studies (*7*, *12*−*14*). Little is understood, however, about the nature of the transition that separates the initial partially folded molten globule form from the completely unfolded form on the folding pathway. Thermodynamic studies of equilibrium molten globules have been unable to resolve explicitly whether the transition between the completely unfolded and molten globule forms is a first- or higher-order transition (*15*, *16*). Moreover, although their temporal resolution has now improved sufficiently to cover the relevant time domain (*17*), kinetic studies still lack the structural resolution to allow a detailed analysis of the steps leading to the formation of molten globule (*18*). Elucidation of these steps in structural detail is vital to an understanding of the conformations that are accessible for sampling by a polypeptide chain as it folds to a molten globule on its route to the native state.

The 89 amino acid residue protein barstar has proven to be a useful model protein to study the initial steps in protein folding. In marginally stable refolding conditions, a hydrophobic collapse has been shown to precede formation of specific structure (*19*), and molten globule-like intermediate forms are populated not only at equilibrium (*20*, *21*) but also transiently on the major folding pathway (*22*, *23*). Barstar provides an unique opportunity for developing an equilibrium model for the steps that lead to the formation of a molten globule because (1) it can be completely unfolded in the absence of chemical denaturant at high pH and (2) a suitable manipulation of solvent conditions can be used to enable formation of a molten globule from the completely unfolded form under equilibrium conditions.

Here, equilibrium studies have been used in conjunction with kinetic studies of a mutant form of barstar, W38FW44F, which contains a single Trp, Trp53, in the core of the fully folded protein, to study the mechanism of formation of a molten globule that populates the direct folding pathway. Barstar has a charge of −18 at pH 12. The electrostatic repulsions between the negative charges keep the high-pH-unfolded D form as expanded as the high-urea-unfolded U form (*24*, *25*). The ability of a salt such as Na_2SO_4 to shield electrostatic interactions when added at low (<0.1 M) concentrations has been exploited to minimize the electrostatic repulsions, so as to drive the D form into a collapsed P form. It is shown that the P form has near-native compactness but no specific secondary or tertiary structure. Then, the well-known ability of Na_2SO_4 to strengthen hydrophobic interactions (*26*), when added at high concentrations, has been exploited to drive the collapsed P form into the molten globule B form. It is shown that the transition from the P to B form is highly noncooperative. Finally, kinetic studies, in which the fluorescence of Trp53 has been used to monitor folding, have been used to demonstrate that

[†] This work was supported by the Tata Institute of Fundamental Research, and the Department of Science and Technology, Government of India. J.B.U. is the recipient of a Swarnajayanti Fellowship from the Government of India.

* Correspondence should be addressed to this author. E-mail: jayant@ncbs.res.in. Fax: 91-80-3636662.

10.1021/bi0120300 CCC: $22.00
Published on Web 01/17/2002

the B form is populated on the direct pathway of folding from the D form to the N state.

MATERIALS AND METHODS

Protein Purification. The double tryptophan mutant of barstar, W38FW44F, was purified using the procedure described earlier (*20*). The purity of the protein was confirmed by SDS−PAGE and MALDI-TOF mass spectrometry, and was found to be >98% pure. Mass spectrometry was also used to verify that the protein was not chemically modified by exposure to pH 12.

Buffers. All reagents used to make buffers were of the highest purity grade; 30 mM sodium tetraborate, 250 μM EDTA, and 0−1 M Na_2SO_4 were the principal buffer components. DTT was used in 50-fold molar excess of protein concentration. The pH was adjusted to 12 using NaOH. Urea-induced unfolding of the protein equilibrated at pH 12 with different Na_2SO_4 concentrations was carried out by equilibrating the samples with increasing urea concentrations. Refractive indices were determined using an Abbe-type refractometer (Milton Roy). Spectroscopic measurements were carried out after 3 h as well as after 24 h of incubation. All buffer solutions were filtered through 0.22 μm filters before use. Protein concentrations used were typically 2 μM for fluorescence, 20 μM for far-UV CD and SEC, and 400 μM for near-UV CD and DLS. All experiments were performed at 25 °C, and over a 10-fold range of protein concentrations to rule out any concentration dependence.

Spectroscopic Methods. Far- and near-UV CD measurements were carried out on a Jasco J-720 spectropolarimeter using a 1 mm path length cuvette. Intensities were obtained at 222 and 275 nm, and averaged over 60 s. Spectra were collected in the 200−250 nm as well as the 250−300 nm range, with a step resolution of 0.1 nm, a scan speed of 20 nm/min, and a bandwidth of 1 nm. Each spectrum was averaged over 10 scans. Fluorescence intensities at 320 nm were obtained on a SPEX fluorolog spectrofluorometer by exciting the sample at 295 nm. Spectra were recorded from 300 to 400 nm, with a scan speed of 1 nm/s and excitation and emission bandwidths of 5 nm. Each spectrum was averaged over 5 scans.

Hydrodynamic Methods. DLS experiments were carried out on a DynaPro-99 unit (Protein Solutions Ltd.). Samples were incubated for 3 h in buffers at pH 12 containing 0−1 M Na_2SO_4. The samples were degassed, spun down at 14 000 rpm for 15 min, and filtered through 0.02 μm filters. Data were acquired over 150 s, where each data point was averaged over 3 s at a sensitivity of 80%. All fluctuations in scattering intensities greater than 15% were excluded from data analysis. The DynaLS software (Protein Solutions Ltd.) was used to resolve the measurements into well-defined Gaussian distributions. The goodness of fit was verified by the residuals. Viscosities of solutions were determined from measured refractive indices.

Data Analysis. The equations used for a three-state, P $\rightleftharpoons$ I_B $\rightleftharpoons$ B, analysis of the Na_2SO_4-induced structural transformation of protein from the P to the B form have been described previously (*27*). In this analysis, the free energy changes ΔG_{IP} and ΔG_{BI}, which characterize the I $\rightleftharpoons$ P and B $\rightleftharpoons$ I equilibria, respectively, are assumed to have linear dependences on Na_2SO_4 concentration.

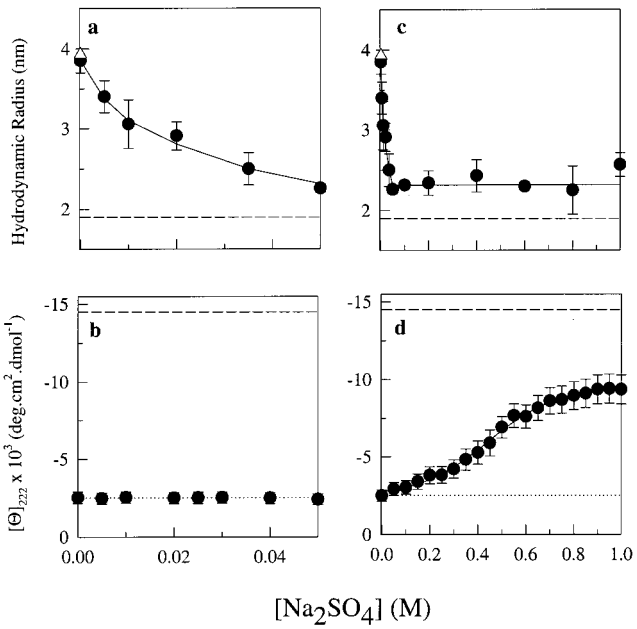

FIGURE 1: Collapse precedes secondary structure formation. (a, c) Hydrodynamic radius of the salt-induced forms at pH 12 as monitored by DLS, plotted as a function of Na_2SO_4 concentration. The dashed line at 1.9 nm corresponds to the hydrodynamic radius of native protein at pH 7. (△) represents the hydrodynamic radius for the U form at pH 7, 6 M GdnHCl. (b, d) Salt-induced changes in the mean residue ellipticity at 222 nm for the D form. The dashed line is the value for native protein at pH 7. The dotted line is the value for the U form in 8 M urea at pH 7. The values represent the averages, and the error bars represent the standard deviations from three separate experiments.

The linear dependence of the free energy of stability on Na_2SO_4 concentration follows from the mode of stabilization by Na_2SO_4 being through a preferential exclusion mechanism (*26*). Similarly, the free energy of activation of any elementary step of the folding mechanism is expected to have a linear dependence on Na_2SO_4 concentration; consequently, for each elementary step, log(rate constant) is expected to depend linearly on Na_2SO_4 concentration.

RESULTS AND DISCUSSION

Collapse of the Polypeptide Chain. Dynamic light scattering (DLS) measurements show that the N state of barstar at pH 7 has an effective hydrodynamic radius of 1.90 ± 0.05 nm, a value similar to that obtained previously from time-resolved anisotropy decay measurements (*28*). Figure 1a shows that the D form at pH 12 has a hydrodynamic radius of 3.9 ± 0.15 nm, similar to that of the U form in 6 M GdnHCl at pH 7, and that upon addition of 0.05 M Na_2SO_4, the D form collapses into a pre-molten globule, or P form, with a hydrodynamic radius of 2.35 ± 0.15 nm. Figure 1b shows that no change in the far-UV CD occurs upon addition of 0.05 M Na_2SO_4, and that the P form, whose volume exceeds that of the N state by only 20%, resembles the D and U forms in being devoid of any specific secondary structure. Size-exclusion chromatography (SEC) measurements show that the P form is more compact than the D form: the elution volumes for the D form at pH 12, the P form at pH 12 in 0.05 M Na_2SO_4, and the N state at pH 7 were 15, 16.8, and 16.8 mL, respectively, on a Superose 6 column. These results confirm the results of the DLS measurements that the P form has near-native compactness.

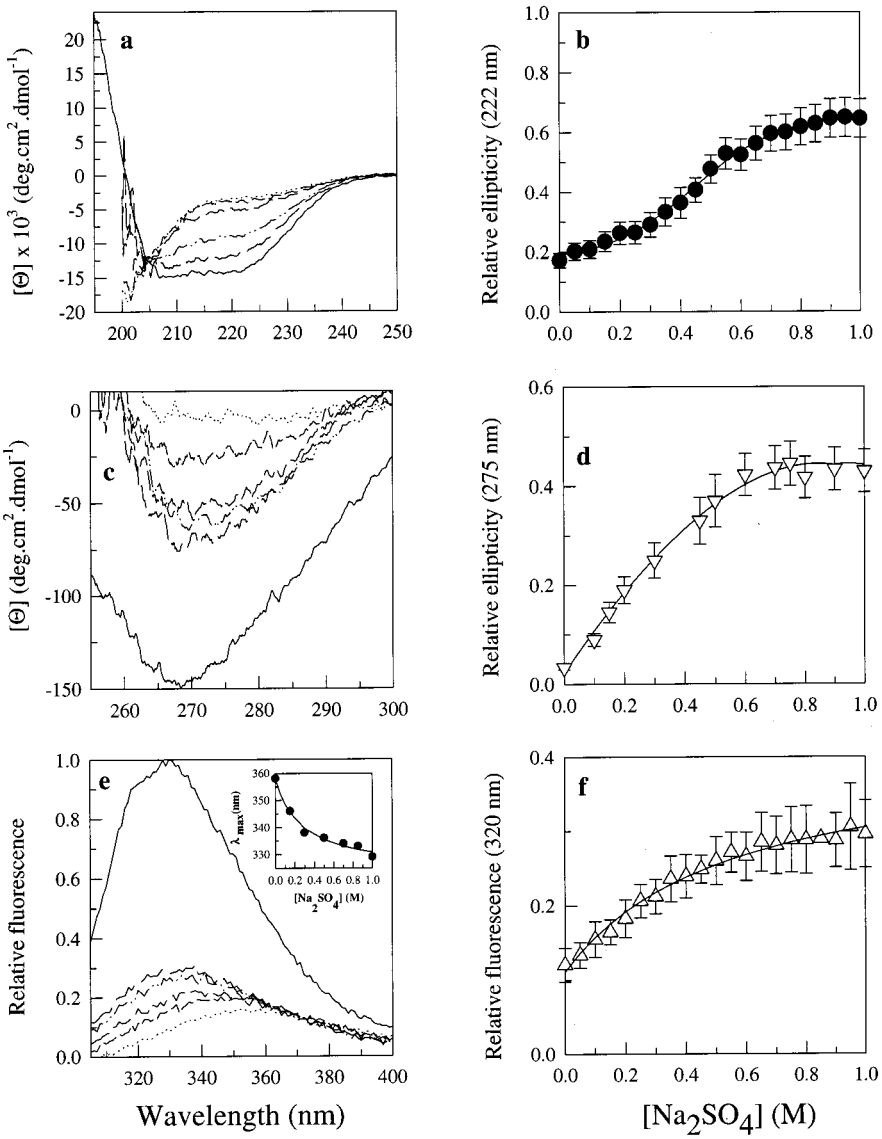

FIGURE 2: Spectroscopic characterization of the pre-molten globule to molten globule transition. (a) Dependence of mean residue ellipticity on wavelength in the peptide region as a function of Na_2SO_4 concentration. The solid line represents the native protein spectrum with maxima at 208 and 220 nm. (b) Relative ellipticity at 222 nm plotted as a function of Na_2SO_4 concentration. (c) Dependence of mean residue ellipticity on wavelength in the aromatic region as a function of Na_2SO_4 concentration. The solid line represents the native protein spectrum with a maximum at 268 nm. (d) Relative ellipticity at 275 nm plotted as a function of Na_2SO_4 concentration. (e) Fluorescence emission spectra recorded as a function of increasing Na_2SO_4 concentration, upon excitation at 295 nm. The solid line represents the native protein spectrum at pH 7, with a λ_{max} at 329 nm. The inset shows the Na_2SO_4 dependence of the λ_{max} of protein. (f) Relative fluorescence of tryptophan at 320 nm plotted as a function of Na_2SO_4 concentration. The dotted lines in panels a, c, and e represent the unfolded protein spectra. Spectra were also obtained after addition of 0.1, 0.25, 0.55, and 1 M Na_2SO_4 to the unfolded protein as shown in panels a, c, and e. All values in panels b, d, and f have been obtained by normalizing to the native protein value.

The intrinsic fluorescence intensity at 320 nm of Trp53 is the same in the P, D, and U forms. Nevertheless, the emission maximum shifts from 357 nm for the D or U forms to 352 nm for the P form, suggesting that Trp53 may not be as completely hydrated in the latter as it is in any of the former. The near-UV CD properties of the P form are similar to those of the D and U forms, suggesting that the P form is indeed a structure-less globule.

The Transition from the Pre-molten Globule P Form to the Molten Globule B Form. Upon a gradual increase in Na_2SO_4 concentration, from 0.05 to 1 M, the polypeptide chain retains the compactness of the P form (Figure 1c), while secondary structure is seen to develop in an apparently cooperative manner (Figure 1d). The P form transforms into the molten globule B form, in 1 M Na_2SO_4. In 1 M Na_2SO_4, the ellipticity at 222 nm of the B form has the same value as does the molten globule-like A form of barstar which forms at pH 3 (*20*). Figure 2a shows that the far-UV CD spectra of the protein in different concentrations of Na_2SO_4 in the range 0.05−1 M exhibit an isodichroic point at 205 nm. This would normally suggest that the P ⇌ B transition is two-state, and Figure 2b shows that the B form achieves 65% of the secondary structure of the N state.

The near-UV CD spectra (Figure 2c) do not display an isodichroic point, and a peak at 270 nm develops progressively upon addition of Na_2SO_4. Figure 2d shows that upon gradually increasing the Na_2SO_4 concentration, the near-UV CD ellipticity at 275 nm increases from a value of near zero (which corresponds to the value of the D, U, and P forms) to a value corresponding to 40% of the value of the N state.

Like for the D and U forms, the P form has an intrinsic tryptophan fluorescence intensity which is about 10% of that of the N state. When the Na_2SO_4 concentration is gradually increased from 0.05 to 1 M, the fluorescence emission spectra show increasing blue shifts (Figure 2e) with the emission maximum changing from 352 nm for the P form in 0.05 M Na_2SO_4 to 330 nm for the B form in 1 M Na_2SO_4 (Figure 2e, inset). Thus, the wavelength of maximum fluorescence emission is the same for the B form and the N state. Throughout the range of Na_2SO_4 concentrations, the fluorescence emission spectra completely overlie each other beyond 360 nm. The intensity of tryptophan fluorescence at 320 nm increases with increasing Na_2SO_4 concentration, from a value in 0.05 M Na_2SO_4 corresponding to 10% of the fluorescence of the N state, to saturate by 0.6 M Na_2SO_4 at a value corresponding to 30% of the fluorescence of the N state. The lower intensity seen for the B form as opposed to that seen for the N state could be due to the lack of defined packing interactions which bring the Asp52 side chain in close proximity to the indole group of Trp53, quenching its fluorescence. All Na_2SO_4-induced structural transitions were found to be completely reversible, and identical results were obtained over a 10-fold range of protein concentration.

Other observations also rule out possible protein aggregation artifacts: (1) negligible aggregation was observed in the DLS experiments at any Na_2SO_4 concentration; (2) no aggregation was observed in SEC experiments at any Na_2SO_4 concentration (data not shown); and (3) time-resolved measurements of the fluorescence anisotropy decay of Trp53 show that the anisotropy decays to zero within 16 ns at any Na_2SO_4 concentration (unpublished results). Since the rotational correlation time of the N state, and also of the B form, is 5.5 ns, this result indicates that there are no high molecular weight forms present, because otherwise longer rotational correlation times would have been observed.

Collapse Precedes Formation of Secondary Structure. The data in Figures 1 and 2 clearly indicate that collapse of the polypeptide chain precedes formation of any specific structure during the salt-induced formation of the molten globule B form of barstar at pH 12. In an earlier study of the folding of barstar in 1 M GdnHCl at pH 7, it had been shown that the initial step of folding was a hydrophobic collapse that was not accompanied by formation of secondary structure, all of which formed afterward (*19*). The measurements carried out here provide direct evidence for the existence of a globally collapsed state devoid of secondary structure, under equilibrium conditions. It is not clear as to what extent subsequent secondary structure formation is facilitated by the collapse, because it must proceed through the rearrangement of groups in a highly viscous interior (*29*). Cytochrome *c* is the only other known example of a protein which can be transformed into a relatively compact form with essentially no secondary structure, albeit by removal of the covalently bound heme group (*30*), but the earliest studied kinetic intermediate on its folding pathway does have significant, although little, secondary structure(*31*).

Noncooperative Nature of the Pre-molten Globule to Molten Globule Transition. When the data in Figure 2 are normalized to a value of 0 for the P form and a value of 1 for the B form (Figure 3), the three structural probes yield nonoverlapping transitions. The two probes used to monitor global tertiary structure, near-UV CD, and intrinsic tryptophan fluorescence yield coincident transitions, while far-UV CD, which provides an estimate of the global secondary structural content, yields a transition curve that is more sigmoidal and which saturates at a higher Na_2SO_4 concentration. Thus, the P ⇌ B transition is not two-state, as suggested by the observation of an isodichroic point (Figure 2a). It appears that the observed isodichroic point occurs purely out of a coincidence of the CD properties of multiple interconverting forms. The data in Figure 3 fit well to a three-state P ⇌ I_B ⇌ B mechanism, where I_B is an intermediate that possesses relatively more of the tertiary structure and relatively less of the secondary structure of the B form. Nevertheless, the data in Figure 3 do not rule out the possibility that I_B represents an ensemble of intermediate forms whose structures change progressively with a change in Na_2SO_4 concentration.

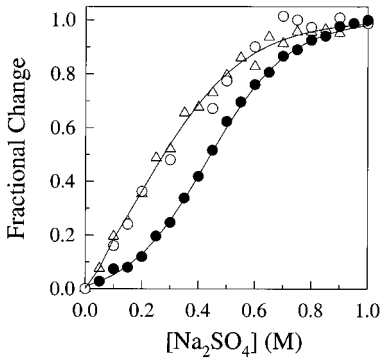

FIGURE 3: Noncooperative nature of the pre-molten globule to molten globule transition. Na_2SO_4-induced changes of ellipticity at 222 (●) and 275 nm (○) and of fluorescence at 320 nm (△) as shown in Figure 2 were normalized to each other. For each spectroscopic probe, the signal, *Y*, at any salt concentration was converted to f_{app}, the fractional change in optical signal, using the equation: $f_{app} = (Y - Y_P)/(Y_B - Y_P)$. Y_P and Y_B represent the signals corresponding to the P form in 0.05 M Na_2SO_4 and the B form in 1 M Na_2SO_4, respectively. The solid lines through the points represent a fit to a P ⇌ I ⇌ B mechanism (*27*).

Is the P ⇌ B Transition a Continuous Transition? To determine whether the Na_2SO_4-induced structural transformation that accompanies the P ⇌ I_B ⇌ B transition involves only one discrete intermediate, I_B, equilibrium urea-induced unfolding curves were determined for the protein incubated in different Na_2SO_4 concentrations at pH 12. Figure 4 compares the far-UV CD-monitored unfolding curves for protein in 0, 0.3, 0.6, and and 1 M Na_2SO_4 at pH 12. No unfolding transition is observed in 0 M Na_2SO_4, and the data for 0 M Na_2SO_4 at pH 12 fall on the linear extrapolation of the unfolding baseline determined for the urea-induced unfolding curve measured at pH 7 (Figure 4, inset), confirming that there is no residual structure in the D form that is dissolved upon addition of urea. When Na_2SO_4 is, however, present, unfolding transitions can be observed, and these transitions occur at higher urea concentrations when higher concentrations of Na_2SO_4 are present. Even in 1 M Na_2SO_4, however, the unfolding curve, which represents the unfolding of the B form, appears to be noncooperative relative to the unfolding curve representing the unfolding of the N state (Figure 4, inset). Moreover, the shapes of the transitions change dramatically, and clearly indicate that the unfolding curves observed in 0.3 and 0.6 M Na_2SO_4 are not the weighted arithmetic sums of the unfolding curves observed in 0 and 1 M Na_2SO_4. Clearly, I_B must represent more than

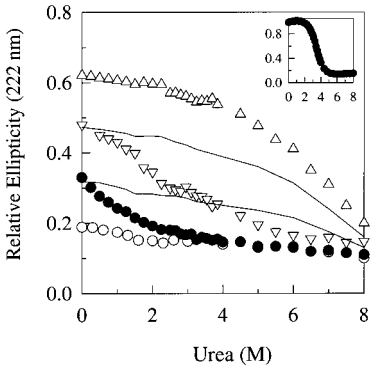

FIGURE 4: Equilibrium urea-induced unfolding of different forms of barstar. Equilibrium unfolding curves were monitored by far-UV CD at 222 nm. The inset shows the cooperative transition of the native protein at pH 7. (○) represents the dependence on urea concentration of the optical properties of the pH 12-unfolded D form. (△), (▽), and (●) represent urea-induced unfolding curves of forms populated in 1, 0.6, and 0.3 M Na_2SO_4, respectively, at pH 12. The solid lines represent the expected titration as obtained from the weighted averages of the optical properties of the D and B forms.

one discrete intermediate state between the P and B forms. Similar results are obtained when intrinsic tryptophan fluorescence is used to monitor the urea-induced unfolding transitions (data not shown).

The B Form Is a Typical Molten Globule. Molten globule forms of proteins are highly dynamic forms with considerable secondary structural elements, relatively few tertiary contacts, and nativelike compactness (*9*, *32*, *33*). The data in Figures 1−4 indicate that the B form of barstar possesses many of these characteristic properties. It is compact, and its volume exceeds that of the N state by only 20%. It has 65% of the secondary structure of the N state as judged by far-UV CD, but very little specific tertiary structure as judged by near-UV CD. It appears that Trp53, which is completely buried in the core of fully folded barstar, is also fully buried in the B form, because water seems to be completely excluded from the vicinity of Trp53 as judged by its intrinsic tryptophan fluorescence spectrum. This could be an indication that the core of the B form is dry, and the B form would therefore qualify as a dry molten globule. It therefore appears that even the small number of tertiary interactions present in the B form results in water being excluded from its hydrophobic core. At the present time, it is not possible to determine whether these tertiary interactions are concentrated in the core. Statistical mechanical models have indicated that a dry molten globule has a collapsed hydrophobic core stabilized by hydrophobic interactions that exclude water from the interior (*34*, *35*), and that such a collapsed form may also induce helical conformations in the polypeptide chain (*34*, *36*). In contrast, the I_B forms resemble more a wet molten globule (see inset, Figure 2e), whose structure is loose enough to allow solvent water to penetrate inside (*37*−*39*).

The B Form Undergoes Noncooperative Unfolding. The urea-induced unfolding curve of the B form of barstar in 1 M Na_2SO_4 at pH 12 is clearly noncooperative (Figure 4), which is most likely due to the absence of specific interactions between secondary structural units. Similarly, the unfolding transition of the human α-lactalbumin molten globule form at pH 2 is also not two-state (*40*). In contrast, the unfolding transitions seen for apomyoglobin (*41*−*43*) and cytochrome *c* (*44*−*46*) molten globules, in which the helices have been shown to interact specifically with nativelike side chain interactions, are highly cooperative. Amino acid substitutions that affect the side-chain packing, and hence the stability of the molten globule form, also change the apparent cooperativity of the unfolding transitions of several proteins (*41*, *44*, *46*−*48*) and suggest that there is a definite correlation between the degree of cooperativity and stability, for the various molten globules.

The Molten Globule Intermediate Is an On-Pathway Intermediate. When either the D or the B form is shifted from pH 12 to pH 7, it folds completely and reversibly to the N state. It is possible to address the important question of whether the B form actually populates the pathway of folding from the D form to the N state, because just as the D form can be fully populated at equilibrium at pH 12 in the absence of any Na_2SO_4, so can the B form be fully populated at equilibrium at pH 12, in the presence of 1 M Na_2SO_4. Both the D and B forms were transferred to identical refolding conditions at pH 7, and their refolding kinetics compared.

A total of 85% of the fluorescence change that occurs during the D → N reaction at pH 7 occurs in a fast phase with a rate constant of 50 ± 5 s^{-1}. With increasing Na_2SO_4 concentration in the final refolding conditions, the observed rate of the fast phase increases in value to saturate at a value of 100 s^{-1} in 0.4 M Na_2SO_4 (Figure 5a), while its relative amplitude remains unchanged at 85%. The nonlinear dependence of log(observed rate) on Na_2SO_4 concentration suggests that at least one intermediate stabilized by Na_2SO_4 populates the folding pathway from D to N (see below). The mechanisms of folding from the D and U forms are similar: the refolding rate at any concentration of GdnHCl in the range 0.6−1.5 M is identical whether refolding is initiated from the D form at pH 12 or from the U form in 8 M urea at pH 7 (data not shown). Salt-induced acceleration of the fast observed rate is also seen when folding is commenced from the 8 M urea-unfolded U form, and is attributed similarly to stabilization of an early folding intermediate by the salt (L. Pradeep and J. B. Udgaonkar, unpublished results).

When the B form in 1 M Na_2SO_4 is shifted from pH 12 to pH 7, it folds completely to the N state; 85% of the fluorescence change that occurs during the B → N reaction occurs in a fast phase with an apparent rate of 120 s^{-1} (Figure 5a), and the observed amplitude as well as rate are independent of the concentration of Na_2SO_4 in the final refolding conditions.

The data in Figure 5a can be analyzed according to a simple D ⇌ B → N mechanism of folding, where the B form is placed as an intermediate on the direct folding pathway. Since the B form is stabilized by the presence of Na_2SO_4, the observed rate of refolding of the D form to the N state is expected to increase with increasing Na_2SO_4 concentration. Conversely, if the B form were an off-pathway intermediate as in a B ⇌ D → N mechanism, the observed rate of refolding of the D form would be expected to decrease with increasing Na_2SO_4 concentration, and the rate of folding of the B form to the N state would never exceed the rate of folding of the D form to the N state. Since the rate of folding of the D form is observed to increase with increasing Na_2SO_4 concentration, and the rate of folding of the B form to

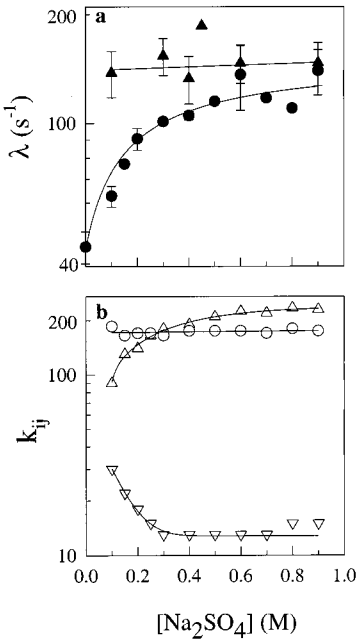

FIGURE 5: Molten globule B form is an on-pathway intermediate. (a) Refolding rates (fast phase) of the pH 12-unfolded D form, when refolded in different concentrations of Na_2SO_4 in the range 0−1 M, at pH 7 (●). Refolding rates (fast phase) of pH 12, 1 M Na_2SO_4 form (B form), when refolded in different concentrations of Na_2SO_4 in the range 0.1−1 M, at pH 7 (▲). The values represent the averages, and the error bars represent the standard deviations from three separate experiments. (b) Microscopic rate constants, k_{ij}, obtained by simulation of the observed rates of the D → N and B → N reactions shown in (a) to the D → B → N mechanism. (△) k_{DB}, the rate constant of the D → B reaction; (▽) k_{BD}, the rate constant of the B → D reaction; (○) k_{BN}, the rate constant of the B → N reaction. The value of k_{NB}, the rate constant of the N → B reaction, has been assumed to be 0.01 s^{-1} at all Na_2SO_4 concentrations. Since the refolding experiments in (a) were carried out at pH 7, the values of the microscopic rate constants in (b) correspond to values at pH 7 only.

the N state exceeds that of the D form to the N state at lower Na_2SO_4 concentrations, it is clear that the B form must be on-pathway. Thus, like the equilibrium molten globule forms of other proteins which also populate direct folding pathways (*1*, *18*, *49*−*53*), the B form of barstar also appears to be populated on the direct folding pathway from the D form to the N state.

Kinetic simulations of the data in Figure 5a, using the KINSIM program (*54*), were used to establish that the D ⇌ B ⇌ N mechanism is indeed valid, and, most importantly, that the alternative B ⇌ D ⇌ N mechanism is not, for the reasons described above. The results of the simulation according to the D ⇌ B ⇌ N mechanism, which accounts for the observed rates when folding is commenced from either the D or the B form, are shown in Figure 5b. As expected, the rate of the D → B reaction increases, and that of the B → D reaction decreases with increasing Na_2SO_4 concentration. The nonlinear dependences of the logarithms of these simulated rate constants on Na_2SO_4 concentration suggests that the D ⇌ B reaction is itself not two-state but multi-state (see Materials and Methods), in support of the equilibrium experiments (Figures 1−4).

Nature of the Transitions from the D Form to the N State. The combination of Na_2SO_4-induced equilibrium folding experiments in which the highly noncooperative structural transformation of the D form to B form has been characterized, and kinetic folding experiments which clearly place the B form as a productive intermediate on the folding pathway of the D form to the N state at high Na_2SO_4 concentrations, allows a structural dissection of the pathway of folding of the D form to the N state into the following steps:

$$D \rightleftharpoons P \rightleftharpoons I_B \rightleftharpoons B \rightarrow N$$

The first step is the collapse of the polypeptide chain to the pre-molten globule P form, whose volume exceeds that of the N state by only 20%, but which is, nevertheless, structure-less. While this first step does not appear to be a cooperative first-order transition, it has not been possible to determine conclusively whether it is indeed a second-order transition. Statistical mechanical models of polymers postulate that the collapse of a random coil into a compact, molten liquid-like state proceeds by a change in second-order derivatives such as heat capacity and compressibility, and is therefore a second-order phase transition (*36*−*38*). It is expected that structural characterization of the P, I_B, and B forms by three-dimensional heteronuclear NMR methods (*55*), now in progress, will allow a better understanding of these higher-order transitions.

The pre-molten globule P form then transforms to the molten globule B form, by a noncooperative structural transition, which has been shown to involve at least two members of what is likely to be a large intermediate ensemble, I_B. Thus, the transformation of the P form to the B form appears to be a higher-order transition such as those seen for homopolymers, which have multiple energy minima to reside in, making the transitions appear continuous (*38*). The transition from the molten globule B form to the N state appears to be a first-order transition, where the two forms are separated by a defined energy barrier.

ACKNOWLEDGMENT

We thank M. K. Mathew, S. Mayor, and R. Varadarajan for discussions.

REFERENCES

1. Kuwajima, K., Hiraoka, Y., Ikeguchi, M., and Sugai, S. (1985) *Biochemistry 24*, 874−881.
2. Kuwajima, K., Yamaya, H., Miwa, S., Sugai, S., and Nagamura, T. (1987) *FEBS Lett. 221*, 115−118.
3. Chaffotte, A. F., Cadieux, C., Guillou, Y., and Goldberg, M. E. (1992) *Biochemistry 31*, 4303−4308.
4. Goldberg, M. E., Semisotonov, G. V., Frituet, B., Kuwajima, K., Ptitsyn, O. B., and Sugai, S. (1990) *FEBS Lett. 263*, 51−56.
5. Sugawara, T., Kuwajima, K., and Sugai, S. (1991) *Biochemistry 30*, 2698−2706.
6. Kuwajima, K., Garvey, E. P., Finn, B. E., Matthews, C. R., and Sugai, S. (1991) *Biochemistry 30*, 7693−7703.
7. Dolgikh, D. A., Gilmanshin, R. I., Brazhnikov, E. V., Bychkova, V. E., Semisotonov, G. V., Venyamnov, S. Y., and Ptitsyn, O. B. (1981) *FEBS Lett. 136*, 311−315.
8. Goto, Y., and Fink, A. L. (1989) *Biochemistry 28*, 945−952.
9. Kuwajima, K. (1989) *Proteins: Struct., Funct., Genet. 6*, 87−103.
10. Ohgushi, M., and Wada, A. (1983) *FEBS Lett. 164*, 21−24.
11. Ptitsyn, O. B. (1992) in *Protein Folding* (Creighton, T. E., Ed.) pp 243−300, W. H. Freeman, New York.
12. Dill, K. A., and Stigter, D. (1995) *Adv. Protein Chem. 46*, 59−104.

13. Finkelstein, A. V., and Shakhnovich, E. I. (1989) *Biopolymers 28*, 1681−1689.
14. Chan, H. S., and Dill, K. A. (1991) *Annu. Rev. Biophys. Biophys. Chem. 20*, 447−490.
15. Griko, Y. V., Freire, E., and Privalov, P. L. (1994) *Biochemistry 33*, 1889−1899.
16. Gittis, A. G., Stites, W. E., and Lattman, E. E. (1993) *J. Mol. Biol. 232*, 718−724.
17. Eaton, W. A., Munoz, V., Hagen, S. J., Jas, G. S., Lapidus, L. J., Henry, E. R., and Hofrichter J. (2000) *Annu. Rev. Biophys. Biomol. Struct. 29*, 327−359.
18. Jennings, P. A., and Wright, P. E. (1993) *Science 262*, 892−896.
19. Agashe, V. R., Shastry, M. C., and Udgaonkar, J. B. (1995) *Nature 377*, 754−757.
20. Khurana, R., and Udgaonkar, J. B. (1994) *Biochemistry 33*, 106−115.
21. Swaminathan, R., Periasamy, N., Udgaonkar, J. B., and Krishnamoorthy, G. (1994) *J. Phys. Chem. 98*, 9270−9278.
22. Shastry, M. C., and Udgaonkar, J. B. (1995) *J. Mol. Biol. 247*, 1013−1027.
23. Sridevi, K., Juneja, J., Bhuyan, A. K., Krishnamoorthy, G., and Udgaonkar, J. B. (2000) *J. Mol. Biol. 302*, 479−495.
24. Khurana, R., Hate, A. T., Nath, U., and Udgaonkar, J. B. (1995) *Protein Sci. 4*, 1133−1144.
25. Rami, B. R., and Udgaonkar, J. B. (2001) *Biochemistry 40*, 15267−15279.
26. Timasheff, S. N. (1998) *Adv. Protein Chem. 51*, 355−432.
27. Nath, U., and Udgaonkar, J. B. (1995) *Biochemistry 34*, 1702−1713.
28. Swaminathan, R., Nath, U., Udgaonkar, J. B., Periasamy, N., and Krishnamoorthy, G. (1996) *Biochemistry 35*, 9150−9157.
29. Chan, H. S., and Dill, K. A. (1990) *Proc. Natl. Acad. Sci. U.S.A. 87*, 6388−6392.
30. Hamada, D., Hoshino, M., Kataoka, M., Fink, A. L., and Goto, Y. (1993) *Biochemistry 32*, 10351−10358.
31. Akiyama, S., Takahashi, S., Ishimori, K., and Morishima (2000) *Nat. Struct. Biol. 7*, 514−520.
32. Kuwajima, K. (1996a) *FASEB J. 10*, 102−109.
33. Ptitsyn, O. B. (1995) *Adv. Protein Chem. 47*, 83−229.
34. Dill, K. A. (1990) *Biochemistry 29*, 7133−7155.
35. Ptitsyn, O. B. (1995a) *Curr. Opin. Struct. Biol. 5*, 74−78.
36. Finkelstein, A. V., and Shakhnovich, E. I. (1989) *Biopolymers 28*, 1681−1689.
37. Shakhnovich, E. I., and Finkelstein, A. V. (1989) *Biopolymers 28*, 1667−1680.
38. Lifshitz, I. M., Grosberg, A. Y., and Khokhlov, A. R. (1978) *Rev. Mod. Phys. 60*, 683−713.
39. Chan, H. S., and Dill, K. A. (1991) *Annu. Rev. Biophys. Biophys. Chem. 20*, 447−490.
40. Nishii, I., Kataoka, M., and Goto, Y. (1995) *J. Mol. Biol. 250*, 223−238.
41. Luo, Y., Kay, M. S., and Baldwin, R. L. (1997) *Nat. Struct. Biol. 4*, 925−930.
42. Kay, M. S., and Baldwin, R. L. (1996) *Nat. Struct. Biol. 3*, 439−445.
43. Kay, M. S., Ramos, C. H. I., and Baldwin, R. L. (1999) *Proc. Natl. Acad. Sci. U.S.A. 96*, 2007−2012.
44. Marmorino, J. L., and Pielak, G. J. (1995) *Biochemistry 34*, 3140−3143.
45. Colon, W. A., Elove, G. A., Wakem, L. P., Sherman, F., and Roder, H. (1996) *Biochemistry 35*, 5538−5549.
46. Marmorino, J. L., Lehti, M., and Pielak, G. J. (1996) *J. Mol. Biol. 275*, 379−388.
47. Shortle, D., and Meeker, A. K. (1989) *Biochemistry 28*, 936−944.
48. Uversky, V. N., Karnoup, A. S., Segel, D. J., Seshadri, S., Doniach, S., and Fink, A. L. (1998) *J. Mol. Biol. 278*, 879−894.
49. Kuwajima, K., Yamaya, H., Miwa, S., Sugai, S., and Nagamura, T. (1987) *FEBS Lett. 221*, 115−118.
50. Ikeguchi, M., Kuwajima, K., Mitani, M., and Sugai, S. (1986a) *Biochemistry 25*, 6965−6972.
51. Baldwin, R. L. (1993) *Curr. Opin. Struct. Biol. 3*, 84−91.
52. Kuwajima, K. (1996b) in *Circular dichroism and the conformational analysis of bio-molecules* (Fasman, G. D., Ed.) pp 159−182, Plenum Press, New York.
53. Arai, M., Ikura, T., Semisotnov, G. V., Kihara, H., Amemiya, Y., and Kuwajima, K. (1998) *J. Mol. Biol. 275*, 149−162.
54. Barshop, B. A., Wrenn, R. F., and Frieden, C. (1983) *Anal. Biochem. 130*, 134−145.
55. Bhavesh, N. S., Panchal, S. C., and Hosur, R. V. (2001) *Biochemistry 40*, 14727−14735.

BI0120300